

## HIGH-TEMPERATURE OXIDATION PROPERTIES OF IRON ALUMINIDES WITH Zr ADDITION

Pavel KEJZLAR, Adam HOTAŘ

Technical University of Liberec, Liberec, Czech Republic, EU, [pavel.kejzlar@tul.cz](mailto:pavel.kejzlar@tul.cz)

### Abstract

Iron aluminides are known for their excellent oxidation and corrosion resistance. If they are exposed to hostile environment, a protective Al<sub>2</sub>O<sub>3</sub> layer creates on its surface. Through an addition of Zr, their high temperature mechanical properties could be enhanced, however, their oxidation resistance is also affected. A small amount of Zr enhances the high temperature oxidation resistance, but at higher concentration it creates ZrO<sub>2</sub> which has a detrimental effect on the oxidation behaviour.

**Keywords:** Intermetallics, oxidation, structure, iron aluminides

### 1. INTRODUCTION

Remarkable oxidation and corrosion resistance of iron aluminides makes them potential candidates to replace nickel-chromium-based stainless steels in high-temperature structural applications [1-6]. However, iron aluminides suffer also from some disadvantages, e.g. insufficient mechanical strength at elevated temperatures (over 600 °C), brittleness at room temperature and the associated poor machinability.

In the last years, considerable research effort has been devoted to an attempt to increase the high temperature mechanical properties [7-11]. It has been shown, that increase in yield stress could be achieved for example by a third element addition. A suitable method to improve the mechanical strength of the iron aluminides appears hardening by secondary phases such as carbides, nitrides, oxides or intermetallic phases. Significant increase in strength was achieved through alloying with elements involved in the formation of very hard and stable Laves phases [12-15].

Due to very limited solubility of Zr in Fe-Al, even a small addition of Zr leads to precipitation of Laves phase and/or  $\tau_1$  phase [16-18]. Presence of these phases enhances mechanical strength but however, it reduces ductility and machinability [19-22]. It has been shown, that a small amount of Zr can eliminate the Al<sub>2</sub>O<sub>3</sub> scales spalling, but higher amount of Zr showed detrimental effect on high temperature oxidation resistance due to formation of ZrO<sub>2</sub> which disrupts the Al<sub>2</sub>O<sub>3</sub> barrier protective function [20, 23-26].

In the present paper the oxidation resistance at 900 °C of Fe-30Al-xZr alloys (where x = 0.4, 0.9 and 5.2 at. %) was evaluated and compared to the results obtained for similar alloys. Also the structure of alloys after 500 exposition was studied and described.

### 2. EXPERIMENTAL

The chemical composition of the materials is given in **Table 1**.

**Table 1** Chemical composition of investigated alloys

| Alloy | Al [at. %] | Zr [at. %] | Fe [at. %] |
|-------|------------|------------|------------|
| 30_0  | 29.3       | 0.4        | Bal.       |
| 30_1  | 29.2       | 0.9        |            |
| 30_5  | 30.1       | 5.2        |            |

Cylindrical samples with diameter of 7 mm and height of 19 mm for testing of oxidation resistance were cut by the electro-discharge machining, their surface was subsequently manually polished by SiC paper grit 1200.

Cyclical oxidation tests were performed in an electric furnace at 900 °C in alumina crucibles. Heating and cooling between individual cycles was realized slowly in the furnace to minimize spallation of the oxide scales. The samples were weighted before tests and after 25, 50, 100, 200, 300, 400 and 500 hours. Measured weight increases were then related to the area units. The oxidation resistance was then calculated as a parabolic rate constant ( $k_p$ ) according to equation (1):

$$(\Delta m/A)^2 = k_p t, \quad (1)$$

where  $\Delta m$  [mg] is a mass increase,  $A$  [cm<sup>2</sup>] is the sample surface area,  $t$  [s] is time. The  $k_p$  values were calculated from  $t = 200$  h.

The structure of samples in both, in the as cast state and after 500 h oxidation, was evaluated using optical microscope and scanning electron microscope equipped with an energy-dispersive detector.

### 3. RESULTS

#### 3.1 Structure

The initial structure of alloys in as cast state was described in detail in [21, 22]. The as cast structure was composed of a lamellar eutectic Fe-Al/Laves phase in a Fe-Al matrix.

The structure after 500 h of oxidation at 900 °C is shown in **Fig. 1**. Long-time exposition to 900 °C led to coarsening and coagulation of LP, a part of LP transformed to  $\tau_1$  phase according to equilibrium Fe-Al-Zr diagram [16, 17]. It is obvious, that preferential selective oxidation occurs in Zr-rich Laves phase (bright areas in SEM images). In both, OM and SEM images, the depth of oxidation ingress is visible; the depth grows with Zr content.

In the case of 30\_5 alloy four different areas are clearly visible (see **Fig. 2**). Area I is composed of oxides (Fe<sub>2</sub>O<sub>3</sub>, Al<sub>2</sub>O<sub>3</sub> and ZrO<sub>2</sub>) and shows the depth of oxide penetration. Area II is composed of Fe-Al and shows the depth from which Zr atom diffused into the oxide layer. Two-phase area III is composed of Fe-Al and Laves phase. Quantitative EDS analysis showed lower Al-concentration compared to the three phase IV area. Lower Al content could be explained through the Al-diffusion into the oxide layer similarly as Zr-absence in area II. The difference in Al and Zr diffusion depths corresponds to their different atom diameter.

#### 3.2 Oxidation kinetics

**Table 2** Parabolic rate constants

| Alloy                      | $k_p$ (g <sup>2</sup> cm <sup>-4</sup> s <sup>-1</sup> ), 900 °C |
|----------------------------|--|
| 30_0 (Fe-29.3Al-0.4Zr)     | $6.4 \times 10^{-13}$  |
| 30_1 (Fe-29.2Al-0.9Zr)     | $5.8 \times 10^{-13}$  |
| 30_5 (Fe-30.1Al-5.2Zr)     | $4.1 \times 10^{-11}$  |
| Fe-20Al-0.1Zr <sup>a</sup> | $9 \times 10^{-14}$ [20]   |
| Fe-32Al-0.8Zr <sup>a</sup> | $4 \times 10^{-13}$ [20]   |
| Fe-25Al <sup>a</sup>       | $1.0 \times 10^{-13}$ [27]                                       |

The calculated parabolic mass constants were calculated for a time interval from 200 to 500 hours and are summarized in **Table 2**. For comparison, in the table are also listed values from [20, 27]. It is obvious, that alloys with lower Zr content show very low values of  $k_p$ , while increase in Zr concentration leads to considerable increase in  $k_p$ , what indicates its detrimental effect on the high temperature oxidation resistance. From the  $k$  values it is obvious, that the oxidation resistance grows also with the Al content.

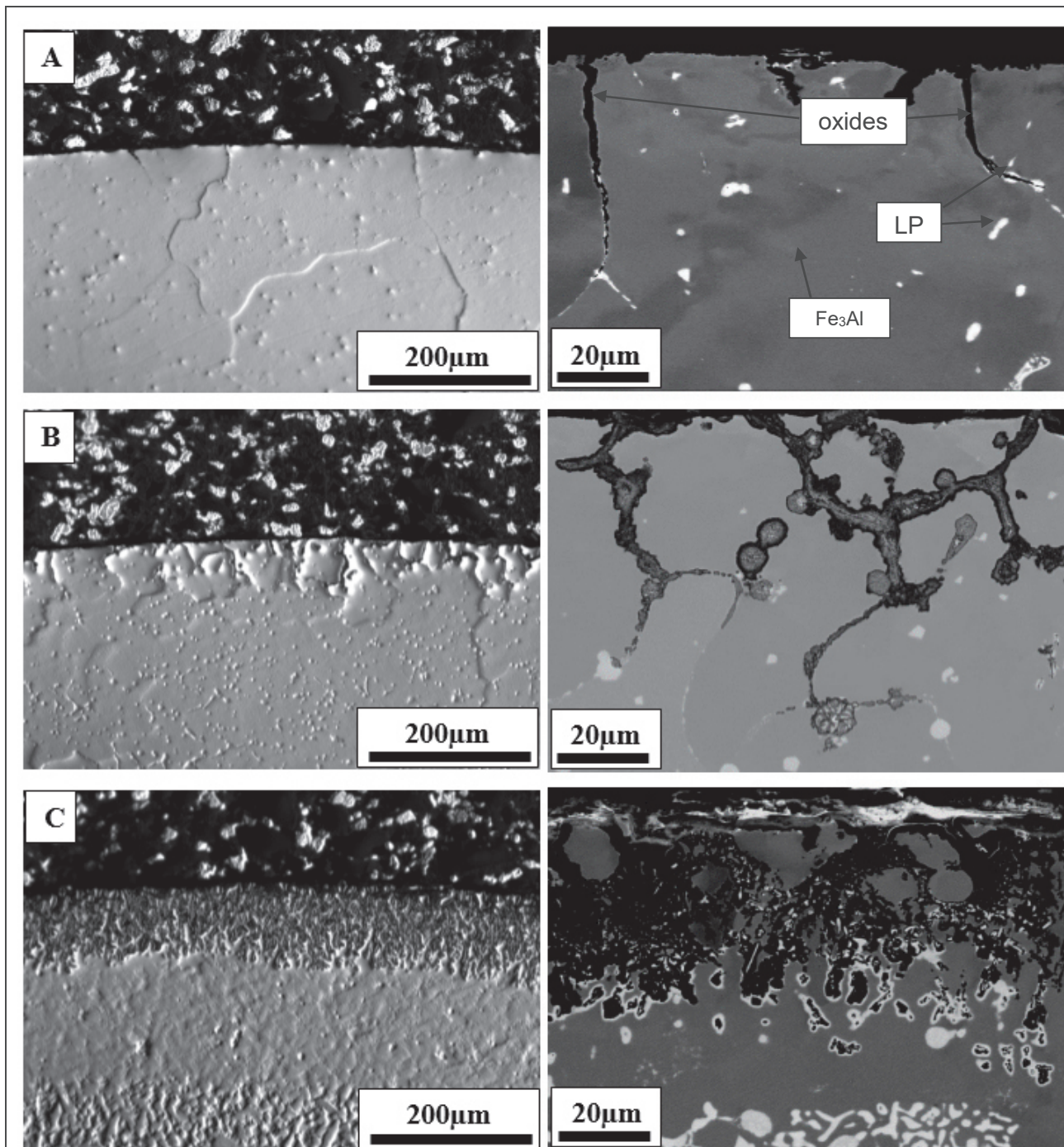


**Fig. 1** Structure of samples oxidized at 900 °C for 500 h. In the left column are images taken by optical microscope, on the right side are SEM images taken in Z-contrast. A) 30\_0 alloy; B) 30\_1 alloy; C) 30\_5 alloy. From the images the ingress of oxidation into the alloys is obvious. The oxidation affects preferentially Zr-containing Laves phase (bright phase in SEM). The depth oxidation ingress grows with Zr content

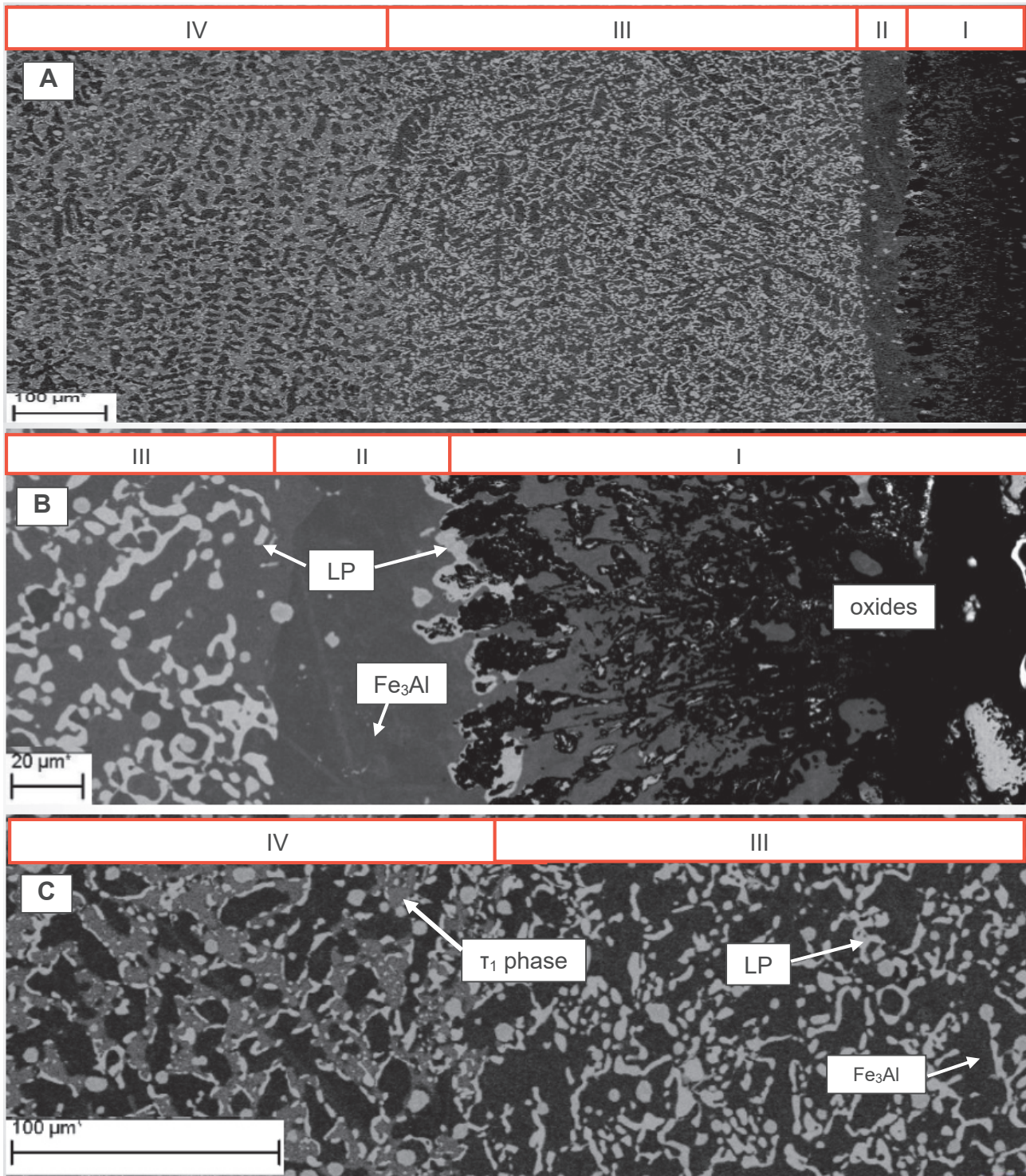


**Fig. 2** Structure of 30\_5 alloy after 500 h at 900 °C

A) Four areas are marked: I. oxidic layer  $\text{Al}_2\text{O}_3 + \text{ZrO}_2$ ; II. Fe-Al; III. Fe-Al + LP; IV. Fe-Al + LP +  $\tau_1$

B) a detail of I/II and II/III boundary

C) Detail of III/IV boundary

## CONCLUSION

After oxidation at 900 °C the inner structure is three-phase. In the Fe-Al matrix occur Laves phase and  $\tau_1$  phase.

With increasing amount of Zr grows the depth of oxidation ingress into the material. The Zr containing Laves phase is oxidized preferentially.

Near the sample surface, four areas were observed. Under the top oxide layer there is Fe-Al area. Then follows a two phase area Fe-Al + LP with lower Al content compared to the inner three phase material where FeAl + LP +  $\tau_1$  phases were identified. Absence of Zr in II-zone and decrease of Al in III-zone could be explained through the diffusion of Zr and Al atoms to the surface to form the oxides.

During the oxidation  $Al_2O_3$  oxide layer forms on the surface. With increasing Zr concentration  $ZrO_2$  appears in the oxide layer. The presence of  $ZrO_2$  in low concentration enhances the  $Al_2O_3$  adhesion, however, in higher amount disrupts its protective/barrier effect and dramatically decreases the high temperature oxidation resistance.

Parabolic rate constants were calculated. While increase of Zr content from 0.4 to 0.9 led to insignificant change in  $k_p$ , the 30\_5 alloy shows nearly two orders of magnitude higher  $k_p$  value what indicates a sharp drop in oxidation resistance.

## ACKNOWLEDGEMENTS

***The results of this project LO1201 were obtained through the financial support of the Ministry of Education, Youth and Sports in the framework of the targeted support of the “National Programme for Sustainability I” and the OPR&DI project Centre for Nanomaterials, Advanced Technologies and Innovation CZ.1.05/2.1.00/01.0005. The research was also supported by the SGS project “Modern Trends in Material Engineering”.***

## REFERENCES

- [1] STOLOFF, N.S., LIU, C.T. *Iron aluminides*. Editor: Li J.C.M. *Microstructure and properties of materials* (Vol. 2). Singapore: World Scientific Publishing Co. Ptc. Ltd., 2000, 139 p.
- [2] DEEVI, S.C., SIKKA, V.K. Nickel and iron aluminides: an overview on properties, processing, and applications. *Intermetallics*, 1996, Vol. 4, p. 357.
- [3] STOLOFF, N.S. Iron aluminides: present status and future prospects. *Materials Science and Engineering A*, 1998, Vol. 258, p. 1.
- [4] TORTORELLI, P.F., DEVAN, J.H. Behavior of iron aluminides in oxidizing and oxidizing/sulfidizing environments. *Materials Science and Engineering A*, 1992, Vol. 153, p. 573.
- [5] DEVAN, J.H., TORTORELLI, P.F. The oxidation-sulfidation behavior of iron alloys containing 16-40 at. % aluminum. *Corrosion Science*, 1993, Vol. 35, p. 1065.
- [6] TORTELLI, P.F., NATESAN, K. Critical factors affecting the high-temperature corrosion performance of iron aluminides. *Materials Science and Engineering A*, 1998, Vol. 258, p. 115.
- [7] MCKAMEY, C.G. et al. Effects of alloying additions on the microstructures, mechanical properties and weldability of  $Fe_3Al$ -based alloys. *Materials Science and Engineering A*, 1994, Vol. 174, p. 59.
- [8] MORRIS, D.G. Possibilities for high-temperature strengthening in iron aluminides. *Intermetallics*, 1998, Vol. 6, p. 753.
- [9] MORRIS-MUNOZ, M.A. Creep deformation of oxide-dispersion-strengthened Fe-40Al intermetallic: thermal and athermal contributions. *Intermetallics*, 1999, Vol. 7, p. 653.
- [10] MORRIS, D.G., MUNOZ-MORRIS, M.A., CHAO, J. Development of high creep resistant iron aluminide. *Intermetallics*, 2004, Vol. 12, p. 821.

- [11] PALM, M. Concepts derived from phase diagram studies for the strengthening of Fe-Al-based alloys. *Intermetallics*, 2005, Vol. 13, p. 1286.
- [12] RISANTI, D.D., SAUTHOFF, G. Strengthening of iron aluminide alloys by atomic ordering and Laves phase precipitation for high-temperature applications. *Intermetallics*, 2005, Vol. 13, p. 1313.
- [13] SCHNEIDER, A. et al. Constitution and microstructures of Fe-Al-M-C (M=Ti, V, Nb, Ta) alloys with carbides and Laves phase. *Intermetallics*, 2003, Vol. 11, p. 443.
- [14] MACHON, L., SAUTHOFF, G. Deformation behaviour of Al-containing C14 Laves phase alloys. *Intermetallics*, 1996, Vol. 4, p. 469.
- [15] ZEUMER, B., SAUTHOFF, G. Intermetallic NiAlTa alloys with strengthening Laves phase for high-temperature applications. I. Basic properties. *Intermetallics*, 1997, Vol. 5, p. 563.
- [16] STEIN, F., SAUTHOFF, G., PALM, M. Phases and phase equilibria in the Fe-Al-Zr system. *Z. Metallkd.*, 2004, Vol. 95, p. 469.
- [17] RAGHAVAN, V. Al-Fe-Zr (Aluminium-Iron-Zirconium). *Journal for Phase Equilibria and Diffusion*, 2006, 27, p. 284.
- [18] WASILKOWSKA, A. et al. Plastic deformation of Fe-Al polycrystals strengthened with Zr-containing Laves phases I. Microstructure of undeformed materials. *Materials Science and Engineering A*, 2004, Vol. 380, p. 9.
- [19] WASILKOWSKA, A. et al. Plastic deformation of Fe-Al polycrystals strengthened with Zr-containing Laves phases Part II. Mechanical properties. *Materials Science and Engineering A*, 2004, Vol. 381, p. 1.
- [20] STEIN, F., PALM, M., SAUTHOFF, G. Mechanical properties and oxidation behaviour of two-phase iron aluminium alloys with  $Zr(Fe,Al)_2$  Laves phase or  $Zr(Fe,Al)_{12}$   $\tau_1$  phase. *Intermetallics*, 2005, Vol. 13, p. 1275.
- [21] KRATOCHVÍL, P. et al. The effect of Zr addition on the structure and high temperature strength of Fe-30 at.% Al alloys. *Intermetallics*, 2012, Vol. 20, p. 39.
- [22] KEJZLAR, P. et al. Phase Structure and High-Temperature Mechanical Properties of Two-Phase Fe-25Al-xZr Alloys Compared to Three-Phase Fe-30Al-xZr Alloys. *Metallurgical and Materials Transactions A*, 2013, Vol. 44, No. 10.
- [23] PRZYBYLSKI, K., CHEVALIER, S., JUZON, P. Effect of Zr on the Oxidation Properties of Fe<sub>3</sub>Al. *Journal of Chinese Society for Corrosion and Protection*, 2009, Vol. 29, p. 286.
- [24] CHEVALIER, S. et al. High-Temperature Oxidation of Fe<sub>3</sub>Al and Fe<sub>3</sub>Al-Zr Intermetallics. *Oxidation of Metals*, 2010, Vol. 73, p. 43.
- [25] XU, C.H., GAO, W., GONG, H. Oxidation behaviour of FeAl intermetallics. The effect of Y and/or Zr on isothermal oxidation kinetics. *Intermetallics*, 2000, Vol. 2, p. 769.
- [26] HOTAŘ, A. et al. High-temperature oxidation behaviour of Zr alloyed Fe<sub>3</sub>Al-type iron aluminide. *Corrosion Science*, 2012, Vol. 63, p. 71.
- [27] POTER, B., STEIN, F., SPIEGEL, M. Microstructure and mechanical properties of directionally solidified Fe-Al-Nb eutectic. *Intermetallics*, 2008, Vol. 16, p. 1212.